



This is a repository copy of *Modeling and simulation framework for hybrid energy storage systems including degradation mitigation analysis under varying control schemes*.

White Rose Research Online URL for this paper:

<https://eprints.whiterose.ac.uk/226609/>

Version: Accepted Version

Proceedings Paper:

Hutchinson, A.J. orcid.org/0000-0002-0342-0989 and Gladwin, D.T. orcid.org/0000-0001-7195-5435 (2022) Modeling and simulation framework for hybrid energy storage systems including degradation mitigation analysis under varying control schemes. In: 2021 International Conference on Electrical, Computer and Energy Technologies (ICECET). 2021 International Conference on Electrical, Computer and Energy Technologies (ICECET), 09-10 Dec 2021, Cape Town, South Africa. Institute of Electrical and Electronics Engineers (IEEE) , pp. 1-6.

<https://doi.org/10.1109/icecet52533.2021.9698815>

© 2021 IEEE. Personal use of this material is permitted. Permission from IEEE must be obtained for all other users, including reprinting/ republishing this material for advertising or promotional purposes, creating new collective works for resale or redistribution to servers or lists, or reuse of any copyrighted components of this work in other works. Reproduced in accordance with the publisher's self-archiving policy.

Reuse

Items deposited in White Rose Research Online are protected by copyright, with all rights reserved unless indicated otherwise. They may be downloaded and/or printed for private study, or other acts as permitted by national copyright laws. The publisher or other rights holders may allow further reproduction and re-use of the full text version. This is indicated by the licence information on the White Rose Research Online record for the item.

Takedown

If you consider content in White Rose Research Online to be in breach of UK law, please notify us by emailing eprints@whiterose.ac.uk including the URL of the record and the reason for the withdrawal request.



eprints@whiterose.ac.uk
<https://eprints.whiterose.ac.uk/>

Modeling and Simulation framework for hybrid Energy Storage Systems including degradation mitigation analysis under varying control schemes

Andrew J. Hutchinson
Electrical and Electronic Engineering
University of Sheffield
Sheffield, United Kingdom
ahutchinson@sheffield.ac.uk

Daniel T. Gladwin, Senior Member, IEEE
Electrical and Electronic Engineering
University of Sheffield
Sheffield, United Kingdom
d.gladwin@sheffield.ac.uk

Abstract— Battery Energy Storage Systems (BESSs) are an increasingly prevalent part of the Great Britain Grid as the energy mix shifts to a higher proportion of intermittent generation such as solar and wind. National Grid ESO (Electricity System Operator) offers a number of frequency response services that can be provided by Energy Storage Systems (ESSs). A significant drawback of BESSs is the degradation experienced when subjected to frequent cycling compared to other energy storage mediums. Modeling and simulation of these systems is key to understanding the impact that hybridization can have on the lifetime and economic viability of such systems. In this paper, a framework for simulation and assessment of the degradation of BESSs offering these services is presented, implementing a micro-cycle-based degradation algorithm and high-resolution data capture of number of cycles occurring at differing C-Rate and SOC ranges. The motivations and methodology behind the method are introduced and discussed and compared with existing methods. The impact of changing hybrid control schemes on battery degradation is introduced and discussed. The framework presented in this paper provides the foundation for further works analyzing the effect of varying control schemes and hybrid configurations on energy storage degradation.

Index Terms— cycle counting, microcycling, simulation, capacity fade, flywheel.

I. INTRODUCTION

Life cycle estimation is a key part of energy storage system design. The effects of energy throughput on a Battery Energy Storage System (BESS) are key to establishing predicted operational lifetimes for different applications. Battery lifetime is usually defined in terms of the maximum number of cycles before failure, where failure is determined as falling to 80% of the original capacity [1]. However, in certain applications such as providing ancillary grid services, it is rare for a BESS to be exposed to a full charge/discharge cycle as shown in Fig.1a. Instead, the ESS moves rapidly through a range of SOC vales as shown in Fig.1b. Microcycling, and the effects of this phenomenon on BESS lifetime has been discussed in previous works such as [2][3][4].

The effects of these partial charges and discharges of the system are commonly referred to as cycle-based degradation generally driven by a combination of factors including the depth of discharge (DoD), state of charge (SoC), C-Rate and energy throughput experienced by the BESS. This is commonly referred to alongside the less variable calendar-driven degradation that is a function of time [5].

Hybrid systems are commonly proposed [6][7] to lower the strain on BESSs, however these systems experience different degradation rates and sensitivity to cycle life when compared

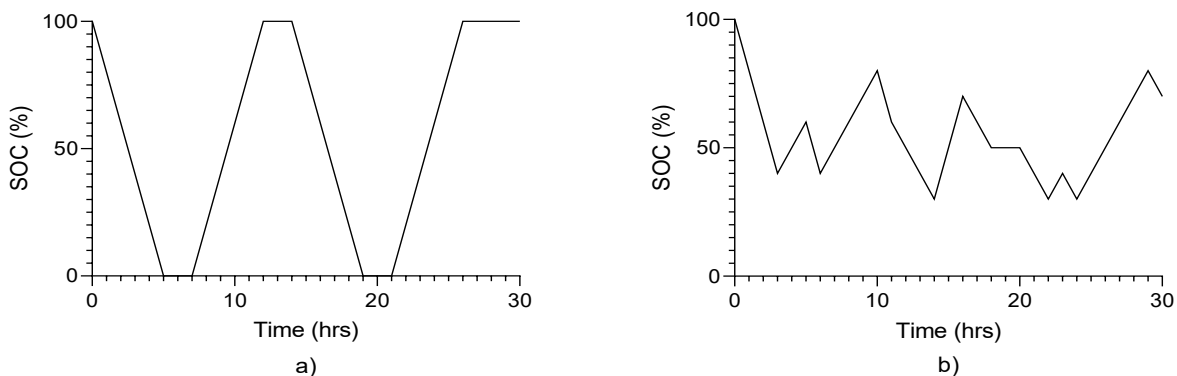


Fig. 1. a) Simple SOC profile representing 2 full charge/discharge cycles b) SOC profile representative of an ESS providing frequency response services showing an example of micro-cycling

to a BESS operating as a standalone system. This paper presents an ESS model representing a BESS operating in tandem with a supplementary Flywheel Energy Storage System (FESS) within MATLAB/Simulink including an improved fast cycle counting method that allows cycles from different energy storage mediums to be directly compared and effective degradation analysis performed. This work also integrates the cycle counting and degradation mechanisms into the overall energy storage system block that is used to simulate performance in providing a frequency response service on the GB grid. Finally, the effect of introducing a FESS as a hybrid system is analysed in terms of effect on battery degradation.

A widespread cycle counting method used in energy storage modeling is called the rain flow algorithm which is commonly used both in energy storage modeling [7][8] and in power electronics [10][11]. The rainflow counting algorithm considers the state of charge as a function of time and applies an algorithm that determines the number of partial cycles that occur at each depth of discharge (DoD). The rainflow algorithm is computationally intensive and can only be applied after the entire period to be studied has been simulated as discussed in [11] and is therefore not suitable for the fast simulation and assessment targeted as part of the framework presented in this paper.

Many papers have discussed and attempted to model the effects of different DoD and SOC on ESS lifetime [12][13][14][15] with differing approaches considered. The work in [15] explores a life cycle model for Li-Ion batteries using equivalent cycle counting. The theory of this method is based upon a set of equations considering DoD, SoC and average C-Rate and converting this calculation into an equivalent cycle. Additionally, [16] and [17] explore degradation of a Li-Ion battery as a direct function of number of cycles and C-Rate, with [17] providing a running % degradation of the overall capacity according to each individual time period.

The foundation for that work is presented in [18] which produced the model from experimental data and is well-suited to usage in fast high-resolution modeling and the overall concept can be used to extract a specific degradation chart for micro-cycle charge/discharge profiles. The work presented in [4] details a cycle counting strategy for MATLAB/Simulink simulations and the research presented in this paper builds upon the work done by refining the method to reduce the computational strain and provide faster and more detailed cycle information. The method presented in this paper details a more granular approach to cycle counting with an estimation accuracy of two decimal places compared to the previous step-based analysis counting only half-cycles.

All examples within this paper are based upon hybrid Battery/Flywheel systems rated as shown in Table I performing a 500kW Dynamic Frequency Response (DFR) service for the Great British Grid over the course of 1 year (using frequency data for 2019 [19]) being modeled and simulated in MATLAB/Simulink. Fig. 2 shows the response envelope for the DFR service, with the dead band between 49.985Hz and 50.015Hz representing the region where no discharging/charging is permitted.

II. CYCLE COUNTING

The method presented in this paper has been developed to provide greater granularity for the number of cycles

experienced during operation to enable a wider range of analysis on how C-Rates, SOC and DoD all affect the degradation of a BESS. Where previously in [4] the cycle counting was conducted so that the cycle number incremented in steps of 0.5 according to a charging and discharging accumulator, this method concentrates solely on total energy throughput for a given second and converts this into an equivalent cycle occurring over a 1s period as shown in (1).

$$\text{Equivalent Partial Cycle} = \frac{|P_{CD}|}{E_c} \quad (1)$$

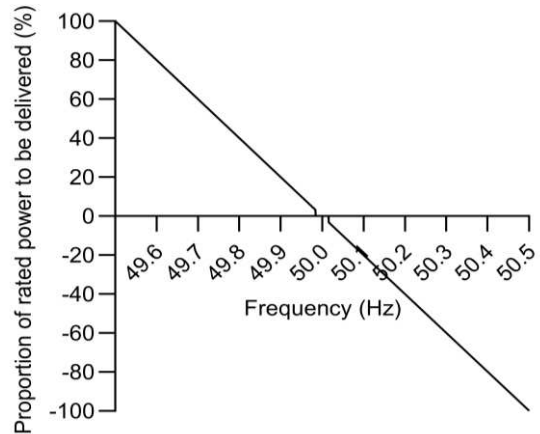


Fig. 2. Frequency response envelope for DFR services in GB.

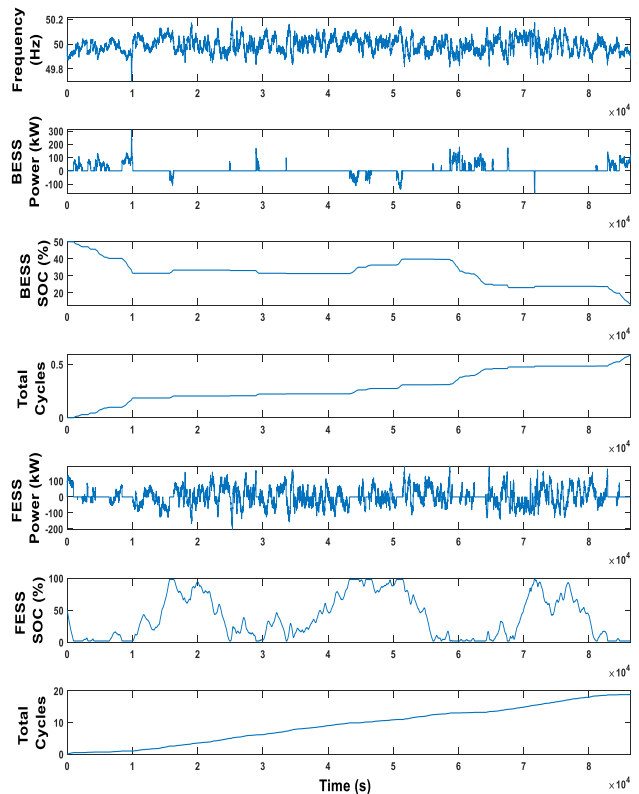


Fig. 3. Demonstration of the cycle counting algorithm in operation for both the BESS and FESS for a 24 hour period delivering a DFR service.

TABLE I. HYBRID ESS POWER/ENERGY RATINGS SHOWING MAXIMUM C-RATE

ESS	kWh	kW	C-Rate
BESS	500	500	1
FESS	50	250	5

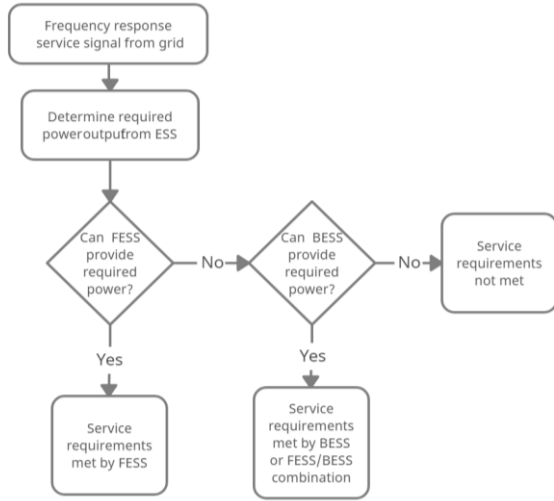


Fig. 4. Control Scheme 1 for Hybrid ESS operation

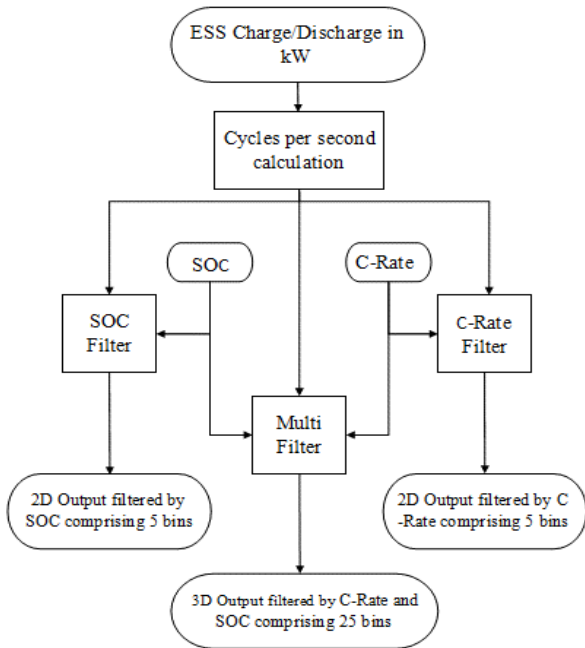


Fig. 5. Filtered analysis algorithm for 5 equal bins of SOC and C-Rate.

Where P_{CD} is the instantaneous charge/discharge from the ESS in kW and E_c is the energy capacity of the ESS in kWh. The output of this, an equivalent cycle for any given second of operation, can then be either continuously integrated to give cycles over the length of the simulation, or used on a second-by-second basis for further analysis. Fig. 3. shows the algorithm in operation for just over one day using frequency data from January 2019, with the cycles counting upward for every individual charge/discharge event that each ESS experiences. From this example, the BESS is shown to only experience 0.6 equivalent cycles whilst the FESS experiences 19.1 equivalent cycles.

The control scheme used to produce these results is a straightforward filter control scheme, illustrated in Fig. 4. The FESS essentially acts as a filter in this control method, attempting to respond to any requests for power, and when it is unable to do so due to high or low SOC, the BESS responds instead.

The flow diagram in Fig. 5. illustrates how the output of this equation can then be filtered further to provide a more

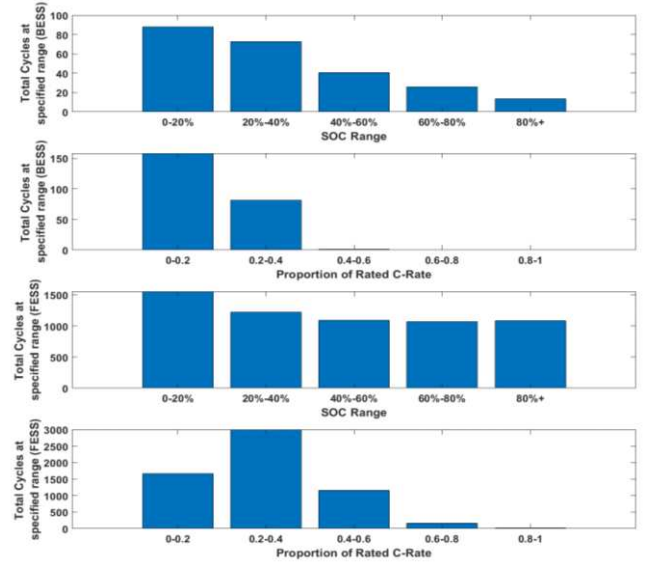


Fig. 6. Filtered number of cycles at differing SOC and C-Rate ranges for BESS and FESS

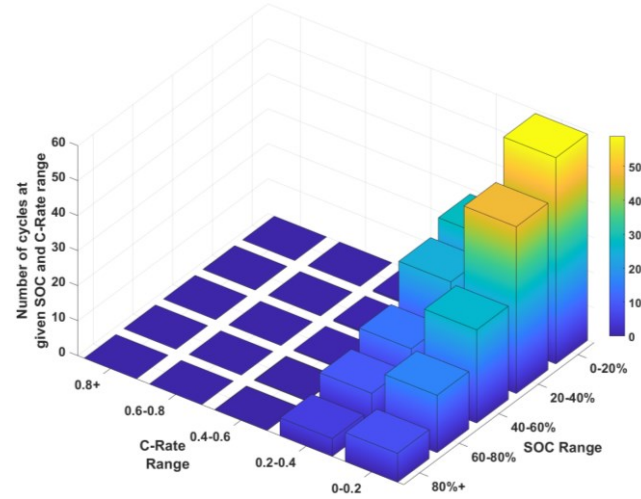


Fig. 7. Total number of cycles at combined ranges of C-Rate and SOC for the BESS under Control Scheme 1

detailed overview of the operation of the ESS. The example shown uses dividers of 0.2/1 when considering C-Rate of the BESS/FESS and 20% when considering either SOC but can be adapted to be as narrow or broad as required. The equivalent partial cycles (EPCs) are summated for each individual bin providing a view of how frequently the ESS is operating within the specified ranges.

This method provides the foundation for further, more detailed assessment of ESS operation as a hybrid system. With the high granularity of the data, research can be performed on tailoring control schemes to keep the ESS operating in certain regions of SOC or C-Rate.

In Fig. 6, the first pass results of the algorithm are presented showing the total number of cycles for both ESS mediums filtered by ranges of SOC and C-Rate at which those cycles occur. This visualization provides an easy method for characterizing the ESS operation, with the FESS clearly operating over a wider range of C-Rates than the BESS, which is restricted to mainly operating in the 0-0.4C range.

To provide further analysis opportunities, Fig. 7 and Fig. 8 illustrate the second level of filter for the BESS and FESS,

respectively. From the analysis presented, both ESSs perform the majority of their cycling at lower C-Rate ranges compared to their overall C-Rating with the FESS operating across the

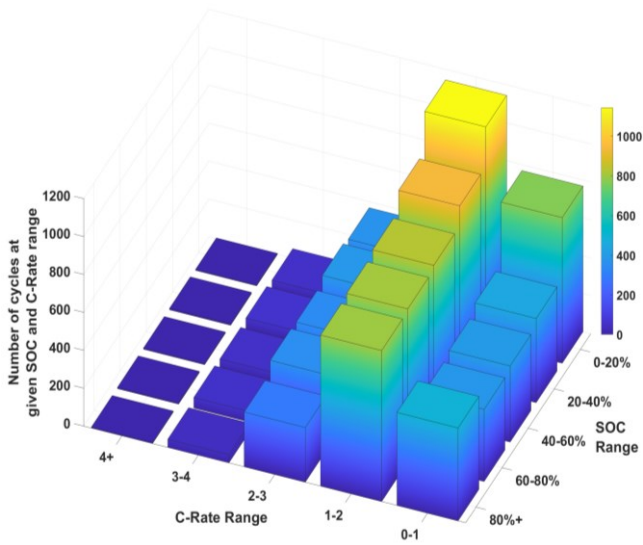


Fig. 8. Total number of cycles at combined ranges of C-Rate and SOC for the FESS under Control Scheme 1

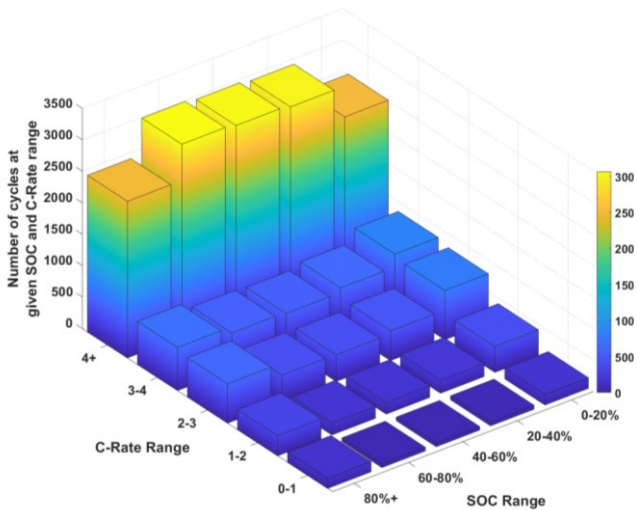


Fig. 9. Total number of cycles at combined ranges of C-Rate and SOC for the FESS under Control Scheme 2

Fig. 10. Total number of cycles at combined ranges of C-Rate and SOC for the BESS under Control Scheme 2

whole spectrum of SOC ranges whilst the BESS tends to operate much more frequently in the 0-40% SOC range which could be detrimental in terms of battery degradation. This visualization of the operation of the system provides a foundation for tailoring the operation of the systems to concentrate the activities of the ESS in specific favorable areas, potentially through the introduction of certain control schemes. In this specific example, the fact that the BESS operates almost exclusively in the 0-0.4C region and the FESS operates over the 0-3C range suggests both aspects of the hybrid ESS may be oversized from a power-rating perspective. Additionally, control schemes could be introduced to manage the SOC in more beneficial ranges for extending battery life as opposed to the low SOC range demonstrated in this analysis.

Control schemes can also have a significant effect on how the BESS operates. Fig. 9 and Fig. 10 show the same presentation of C-Rate and SOC range of operation but this time for an alternative control scheme (Control Scheme 2, Fig. 11), where instead of simply acting as a filter, the Flywheel instead provides a rolling 30-second average of the requested power and the Battery provides the difference between instantaneous requested power and Flywheel output. The impact from this change in control scheme is significant, with the FESS now operating mostly in the 4+ C-Rate range, which suggests the higher power nature of the FESS is utilized to good effect under this control scheme. The BESS (Fig. 10) now operates more evenly across the various SOC ranges when compared to control scheme 1, whilst still being concentrated in the 0-0.4C range of operation. The greater spread of average SOC could prove valuable in maintaining a BESS within manufacturer specified guidelines and is likely to lead to a longer lifespan than when compared to Control Scheme 1.

Alternatively, Fig. 12 & Fig. 13 show the FESS & BESS operational statistics with the Battery providing a response for frequencies between 49.9Hz and 50.1Hz and the Flywheel providing a response for frequencies outside of this range (Control Scheme 3, Table III). For the FESS, the SOC range is still spread evenly across the spectrum whereas the C-Rate

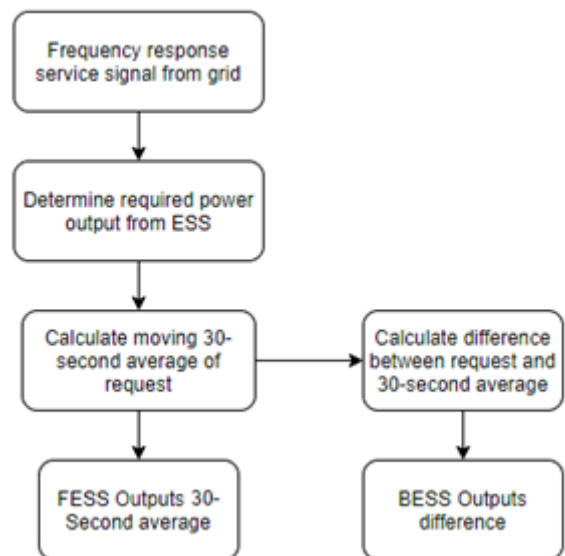


Fig. 11. Control Scheme 2 for Hybrid ESS operation

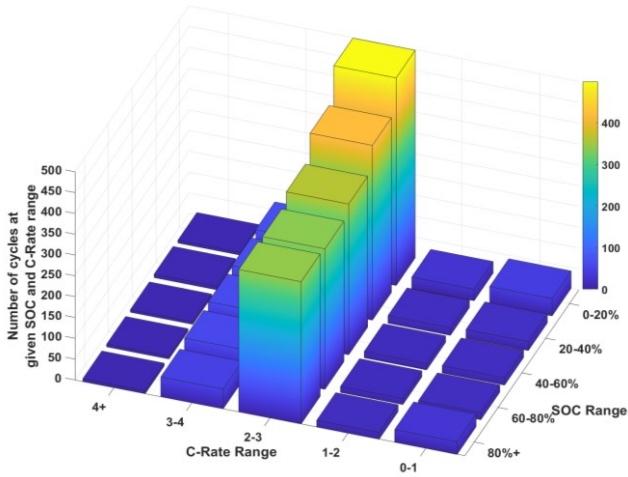


Fig. 12. Total number of cycles at combined ranges of C-Rate and SOC for the FESS under Control Scheme 3

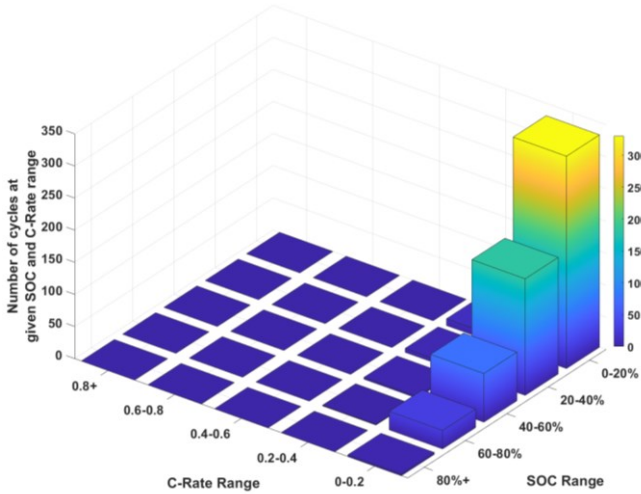


Fig. 13. Total number of cycles at combined ranges of C-Rate and SOC for the BESS under Control Scheme 3

is now almost exclusively maintained in the 2-3 range with a small amount of activity in the other regions. This is because the FESS is providing only the higher-power responses with lower C-Rates largely unutilized. Fig. 12 suggests that the FESS could be more appropriately sized to a 4C system as the higher C-Rate is not utilized effectively. The activity from the battery is now almost exclusively within the 0-0.2 C-Rate with a much larger proportion of the activity also taking place in the 0-20% SOC range. This analysis shows that the battery is significantly oversized for this control scheme and likely could be reduced in size for cost savings.

The control schemes discussed in this section have been derived as part of a series of parallel works looking into the effect of control schemes on hybrid energy storage systems technical and economic viability.

TABLE II. CONTROL SCHEME 3 OPERATIONAL PARAMETERS]

Frequency Range	ESS System used to respond
<49.9Hz	FESS
49.9-50.1Hz	BESS
>50.1Hz	FESS

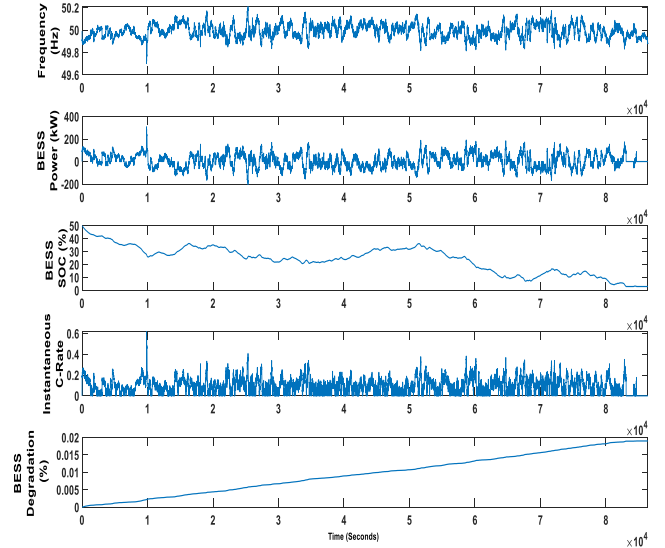


Fig. 14. Simulation results showing the degradation algorithm in operation

III. DEGRADATION MODELING

The equation presented in [18] is used to calculate the incremental degradation for a period Δt as shown in equations (2) – (4).

$$\Delta Q_{loss}^{cycle}(t) = B_1 \cdot e^{B_2 \cdot I_{rate}} \cdot A_h \Delta t \quad (2)$$

$$B_1 = a \cdot T^2 + b \cdot T + c \quad (3)$$

$$B_2 = d \cdot T + e \quad (4)$$

Where the values of a , b , c , d , and e are constants as given in Table II, I_{rate} is the C-Rate for that period, A_h is the energy throughput over that period and T is the temperature. For the purposes of this study, it has been assumed that the energy storage is kept in a temperature-controlled housing unit maintaining 20°C (293K). In this study, all instances of Δt are a 1 second period, with the C-Rate calculated as the rate at which the BESS is asked to charge/discharge over that 1 second period and the energy throughput calculated over the same period. Fig. 14 shows the simulation in operation, with degradation increasing incrementally with each partial cycle. Higher C-Rates and energy throughput causes greater incremental increases in the overall degradation total.

These equations have been represented within MATLAB/Simulink to model the effects of micro-cycle-based degradation with results from a year-long simulation shown in Fig. 15. As expected, there is a significant reduction in degradation when Flywheel Energy Storage is introduced. Both control schemes discussed show a reduction in degradation, with Control Scheme 1 showing the lowest eventual degradation from 1 year of operation. Control Scheme 3 on the other hand has the least impact on degradation rates although it still reduces end of year

TABLE III. COEFFICIENT VALUES AND UNITS FOR DEGRADATION EQUATION [18]

Coefficient values and units	
a	8.61E-6, 1/Ah-K ²
b	-5.13E-3, 1/Ah-K
c	7.63E-1, 1/Ah
d	-6.7E-3, 1/K-(C-rate)
e	2.35, 1/(C-rate)

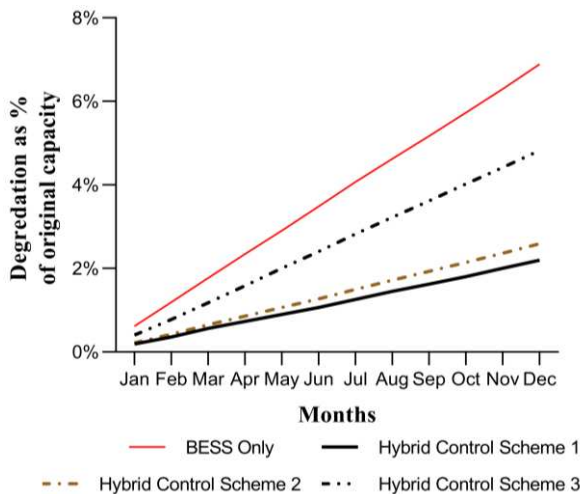


Fig. 15. Degradation as a percentage of original capacity for BESS-Only and hybrid control schemes

degradation from 6.8% to 4.8%, showing the importance of effective control when implementing hybrid energy stores.

IV. CONCLUSION

A framework for modeling energy storage systems and simulating their operation providing frequency response services has been presented. The number of cycles that occur at a range of different SOCs or C-Rates can be determined quickly and effectively for any ESS medium. The framework provides the basis for optimizing battery operation through control strategies and the cycle counting strategy improves upon previous methods through a quicker and more granular result generation. The modeling framework was demonstrated with a hybrid energy storage system showcasing the granularity of equivalent cycle counting within the model. The various visualizations available from this data have been demonstrated, with the FESS within the hybrid system being shown to operate across a wider range of C-Rate values than the BESS.

Secondly, a battery degradation effect was implemented into the model to provide a platform for a more detailed analysis on the benefits of hybridizing battery energy storage with alternative storage technologies. This was then demonstrated as part of the same hybrid ESS model, with the rate of degradation showing a significant reduction when the system was hybridized compared to a BESS operating independently. The algorithm could also be improved upon by considering a variable temperature element as opposed to the constant value specified within this paper.

Finally, different control schemes for hybrid energy storage systems have been introduced and discussed. There is clearly potential for varying control schemes to be exploited to maintain battery operation in optimal ranges for prolonging lifetime, and the importance of choosing the correct control scheme is shown by the varying levels of degradation for each control scheme. A dynamic control scheme could be employed to manipulate battery operation to keep degradation as low as possible whilst still achieving performance objectives.

REFERENCES

[1] B. M. Gundogdu, "Control Analysis for Grid Tied Battery Energy Storage System for SOC and SOH Management," no. April, 2019, [Online]. Available: <http://etheses.whiterose.ac.uk/24593/>.

[2] M. Ceraolo, A. Di Donato, C. Miulli, and G. Pede, "Microcycle-based efficiency of hybrid vehicle batteries," in 2005 IEEE Vehicle Power and Propulsion Conference, VPPC, 2005, vol. 2005, pp. 60–64, doi: 10.1109/VPPC.2005.1554533.

[3] M. Ceraolo, G. Lutzemberger, and D. Poli, "Aging evaluation of high power lithium cells subjected to micro-cycles," *J. Energy Storage*, vol. 6, pp. 116–124, 2016, doi: 10.1016/j.est.2016.03.006.

[4] B. Gundogdu and D. T. Gladwin, "A Fast Battery Cycle Counting Method for Grid-Tied Battery Energy Storage System Subjected to Microcycles," *iEECON 2018 - 6th Int. Electr. Eng. Congr.*, 2018, doi: 10.1109/IEECON.2018.8712263.

[5] M. Ecker et al., "Calendar and cycle life study of Li(NiMnCo)O₂-based 18650 lithium-ion batteries," *J. Power Sources*, vol. 248, pp. 839–851, 2014, doi: 10.1016/j.jpowsour.2013.09.143.

[6] S. D. Sessa, A. Tortella, M. Andriollo, and R. Benato, "Li-ion battery-flywheel hybrid storage system: Countering battery aging during a grid frequency regulation service," *Appl. Sci.*, vol. 8, no. 11, pp. 1–15, 2018, doi: 10.3390/app8112330.

[7] N. R. Tummuru, M. K. Mishra, and S. Srinivas, "Dynamic Energy Management of Renewable Grid Integrated Hybrid Energy Storage System," *IEEE Trans. Ind. Electron.*, vol. 62, no. 12, pp. 7728–7737, 2015, doi: 10.1109/TIE.2015.2455063.

[8] S. You and C. N. Rasmussen, "Generic modelling framework for economic analysis of battery systems," in *IET Conference Publications*, 2011, vol. 2011, no. 579 CP, p. 122, doi: 10.1049/cp.2011.0147.

[9] S. F. Schneider, P. Novak, and T. Kober, "Rechargeable batteries for simultaneous demand peak shaving and price arbitrage business," *IEEE Trans. Sustain. Energy*, vol. 12, no. 1, pp. 148–157, 2021, doi: 10.1109/TSTE.2020.2988205.

[10] L. R. GopiReddy, L. M. Tolbert, B. Ozpineci, and J. O. P. Pinto, "Rainflow Algorithm-Based Lifetime Estimation of Power Semiconductors in Utility Applications," *IEEE Trans. Ind. Appl.*, vol. 51, no. 4, pp. 3368–3375, 2015, doi: 10.1109/TIA.2015.2407055.

[11] A. Antonopoulos, S. Drarco, M. Hernes, and D. Pefitsis, "Challenges and strategies for a real-time implementation of a rainflow-counting algorithm for fatigue assessment of power modules," *Conf. Proc. - IEEE Appl. Power Electron. Conf. Expo. - APEC*, vol. 2019-March, no. March, pp. 2708–2713, 2019, doi: 10.1109/APEC.2019.8722284.

[12] S. Canevese, A. Gatti, E. Micolano, L. Pellegrino, and M. Rapizza, "Battery Energy Storage Systems for frequency regulation: Simplified aging evaluation," in 2017 6th International Conference on Clean Electrical Power: Renewable Energy Resources Impact, ICCEP 2017, 2017, pp. 291–297, doi: 10.1109/ICCEP.2017.8004830.

[13] I. Laresgoiti, S. Käbitz, M. Ecker, and D. U. Sauer, "Modeling mechanical degradation in lithium ion batteries during cycling: Solid electrolyte interphase fracture," *J. Power Sources*, vol. 300, pp. 112–122, 2015, doi: 10.1016/j.jpowsour.2015.09.033.

[14] M. Broussely et al., "Main aging mechanisms in Li ion batteries," *J. Power Sources*, vol. 146, no. 1–2, pp. 90–96, 2005, doi: 10.1016/j.jpowsour.2005.03.172.

[15] S. N. Motapon, E. Lachance, L.-A. Dessaint, and K. Al-Haddad, "A Generic Cycle Life Model for Lithium-Ion Batteries Based on Fatigue Theory and Equivalent Cycle Counting," *IEEE Open J. Ind. Electron. Soc.*, vol. 1, no. August, pp. 207–217, 2020, doi: 10.1109/ojies.2020.3015396.

[16] C. Zhang et al., "Using CPE function to size capacitor storage for electric vehicles and quantifying battery degradation during different driving cycles," *Energies*, vol. 9, no. 11, 2016, doi: 10.3390/en9110903.

[17] D. Wang, J. Coignard, T. Zeng, C. Zhang, and S. Saxena, "Quantifying electric vehicle battery degradation from driving vs. vehicle-to-grid services," *J. Power Sources*, vol. 332, pp. 193–203, 2016, doi: 10.1016/j.jpowsour.2016.09.116.

[18] J. Wang et al., "Degradation of lithium ion batteries employing graphite negatives and nickel-cobalt-manganese oxide + spinel manganese oxide positives: Part 1, aging mechanisms and life estimation," *J. Power Sources*, vol. 269, pp. 937–948, 2014, doi: 10.1016/j.jpowsour.2014.07.030.

[19] National Grid ESO, "Historic Frequency Data," 2021. <https://www.nationalgrideso.com/balancing-services/frequency-response-services/historic-frequency-data> (accessed Feb. 14, 2021).